AIP | The Journal of Chemical Physics

The dissociative recombination rate coefficients of H+ 3, HN+ 2, and HCO+

T. Amano

Citation: The Journal of Chemical Physics **92**, 6492 (1990); doi: 10.1063/1.458594
View online: http://dx.doi.org/10.1063/1.458594
View Table of Contents: http://scitation.aip.org/content/aip/journal/jcp/92/11?ver=pdfcov
Published by the AIP Publishing

The dissociative recombination rate coefficients of H_3^+, HN_2^+, and HCO^+

T. Amano
Herzberg Institute of Astrophysics, National Research Council, Ottawa, Canada K1A 0R6

(Received 24 August 1989; accepted 23 February 1990)

The dissociative recombination rate coefficients for H_3^+, HN_2^+, and HCO^+ are determined at 110, 210, and 273 K by monitoring the decay of the infrared absorption signals as a function of time. The rate coefficients are 1.8, 7.0, and 3.1 in units of 10^{-7} cm^3 s^{-1} for H_3^+, HN_2^+, and HCO^+, respectively, at 273 K. These values agree very well with those obtained using the stationary afterglow or the merged beam techniques, but the values for H_3^+ disagree with that obtained by Smith and co-workers ($\leqslant 2\times 10^{-8}$ cm^3 s^{-1}) using the flowing afterglow/Langmuir probe method. The rate coefficients for H_3^+ and HCO^+ disagree with theory which has predicted very slow dissociative recombinations in the lower vibrational states. The temperature dependences obtained here, although the temperature range is rather limited, are consistent with those obtained previously using the stationary afterglow (for H_3^+ and HCO^+) and the merged beam (for HN_2^+) techniques. The measurements are extended to several vibration–rotation levels and no significant rotation dependence of the rate coefficients is observed. It has also been found that the ions investigated here can be equally abundant at ice temperature as at liquid nitrogen temperature.

I. INTRODUCTION

According to recent work of Adams, Smith, and Alge,[1,2] the dissociative recombination rate coefficient of H_3^+ with electrons is much smaller than values obtained previously. These authors employed the flowing afterglow/Langmuir probe (FALP) technique and obtained a rate coefficient of $\leqslant 2\times 10^{-8}$ cm^3 s^{-1}. Later they[3] revised the value to be even smaller, less than 10^{-11} cm^3 s^{-1}. The dissociative recombination rate coefficients of most positive molecular ions with electrons are known to be of the order of 10^{-6}–10^{-7} cm^3 s^{-1}. As H_3^+ plays a key role in laboratory discharge plasmas, in planetary atmospheres, and in interstellar space, its dissociative recombination rate coefficient has been measured repeatedly using various techniques. Leu, Biondi, and Johnsen[4] determined the rate coefficient to be 2.3×10^{-7} cm^3 s^{-1} at 300 K by using the stationary afterglow (SA) method. More recently, Macdonald, Biondi, and Johnsen[5] obtained a smaller value 1.7×10^{-7} cm^3 s^{-1} at 300 K using a similar microwave afterglow technique. The recombination cross sections were also measured using several other techniques such as the inclined beam,[6] the merged beam (MB),[7,8] and the ion-trap[9] techniques. The cross sections depend on the center-of-mass electron energy or the electron temperature, showing approximately an E_e^{-1} dependence, where E_e is the electron energy. The value obtained with the stationary afterglow method is interpreted to be a thermal rate coefficient which is obtained under the condition of $T_e \simeq T_i \simeq T_{gas}$, whereas the cross sections obtained with the merged beam technique are mostly nonthermal, where $T_e \gg T_i \simeq T_{gas}$. All the cross sections and the rate coefficients obtained by the various techniques referred to above were reasonably consistent after correcting for the different electron energy and the different electron temperature, except for the more recent value obtained by Smith and his co-workers.[1–3]

They ascribed the previous larger values of the rate coefficients to vibrationally excited H_3^+, referring to a theoretical calculation by Michels and Hobbs[10] who showed that H_3^+ in $v\leqslant 2$ states (without specifying the vibrational mode) should have negligibly small dissociative recombination rate coefficients due to the absence of the crossings of the dissociative potential surfaces of H_3. Also recently, Hus *et al.*[11] repeated the merged beam experiments and obtained a cross section which is about an order of magnitude smaller than the previous value determined using a similar technique.[7] They suggested that the ions in the experiment by Auerbach *et al.*[7] were hot and the rate constant of the order of 10^{-7} cm^3 s^{-1} obtained was not the rate for H_3^+ in the ground state, but a value of excited vibrational states (see also a paper by Mitchell *et al.*[12]). Johnsen suggested in his recent review article[13] that the rate coefficients obtained in Refs. 4 and 5 were likely to be flawed by an impurity ion CH_5^+.

Considering the broad impact of these low values, we carried out direct measurements of the decay of the infrared absorption signals and the ion population in a particular vibration–rotation state of H_3^+ produced in a pulse discharge as a function of time, and obtained a rate coefficient of 2×10^{-7} cm^3 s^{-1} for H_3^+ in the $J=3, K=3$ rotational state in the ground vibrational state.[14] Our value agreed with those obtained by the SA[4,5] and MB[7,12] methods which disagreed with the value obtained by Smith and co-workers and were thought to be due to vibrationally excited H_3^+. Since the value did not agree with the most recent result obtained by Smith and co-workers which seemed to be gaining general acceptance, we carefully examined possible causes which might have made our result different from theirs. However, as discussed in Ref. 14, the result could not be reasonably understood in any other way than the dissociative recombination is the process responsible for the decay observed in our experiments. To provide further confirmation, we have extended the measurements to several other vibration–rotation states of H_3^+ and to other ions, namely HN_2^+ and HCO^+, at liquid nitrogen temperature, at dry-ice (-60 °C) and at ice (0 °C) temperatures. These results will

demonstrate the internal consistency of our experimental results.

The dissociative recombination rate coefficient of HCO^+ was measured using the stationary afterglow (SA) technique[15] and the FALP technique.[1,2] The FALP result gave a rate coefficient smaller by a factor of 2 than that obtained by the SA method. The more recent SA measurement[16] confirmed the previous SA result. Mul and McGowan[17] obtained the recombination cross sections for HN_2^+ by the merged beam method. Smith and co-workers[1,2] also determined the rate coefficient for HN_2^+. These results disagree by a factor of 2, but the discrepancy is not so serious compared with the discrepancy for H_3^+.

In addition, the present investigation has provided the data on the temperature dependence of the dissociative recombination rate coefficients in the range of 110–273 K. It was found that the temperature dependence was in good agreement with previous results. In the course of determination of the rate coefficients, the rotational and translational temperatures of the ions produced in the pulse discharge were found to be lower than previously assumed. Also we have found that H_3^+, HN_2^+, and HCO^+ can be generated equally well at ice temperature (0 °C) as at liquid nitrogen temperature.

II. EXPERIMENTAL DETAILS

Figure 1 shows a schematic diagram of the experimental setup. Ions were generated in a cooled hollow cathode by applying pulse discharge and the concentration of an ion was monitored by observing the decay of the infrared absorption signals as a function of time. The frequency of the infrared laser radiation from a difference frequency laser system was held fixed at the center of a particular vibration–rotation transition line. The details of the apparatus were as described in previous papers.[18,19] The laser beam was sent through a hollow cathode discharge cell fitted with a set of multitraversal mirrors. The typical pathlength used in this work was 28.8 m. We used two different cathodes made of stainless steel in the initial stages, one of 38 mm inner diameter and the other of 60 mm inner diameter and both of them of 80 cm in length, to examine if the process is diffusion limited, and, as discussed in Ref. 14, the ambipolar diffusion was found not to be the dominant process. The transmitted laser radiation was received by a liquid nitrogen cooled InSb photovoltaic detector and the signal was amplified with a preamplifier (Infrared Associates, Model PPA-15-IS). The bandwidth of the detector and the preamplifier system was estimated to be about 10 MHz. The decay of the absorption intensity after pulse discharge was recorded with a digital storage oscilloscope (HITACHI VC6050). The stored signals were transferred to a microcomputer (HP 9816) for analysis.

Special care was taken to induce a pulse discharge without ringing in the hollow cathode. The pulse width was 20–40 μs and the repetition frequency was about 1 kHz. An output transformer for transistor circuits (Hammond 147R) mounted in an oil bath was utilized for this purpose (see Fig. 1 of Ref. 14). The discharge was cooled by flowing either cooled methanol or liquid nitrogen through copper tubing soldered onto the outside of the cathode. The temperature of circulated methanol was controlled by a bath circulator (NESLAB ULT-80DD) and the temperature quoted as the cell temperature in the text was the measured bath temperature. In the case of liquid nitrogen cooling, we ensured that a sufficient flow of liquid nitrogen was maintained so that the liquid flow all the way to the exit of the cooling tube. We will discuss the translational and rotational temperatures of the ions in the next section.

H_3^+ was produced in the hollow cathode by discharging 200–600 mTorr of H_2. HN_2^+ and HCO^+ were generated by adding a 20–30 mTorr of N_2 or CO to the H_2 discharge. The hydrogen gas was obtained from a commercial cylinder (Matheson or Linde, ultrahigh-pure grade, 99.999%) and was introduced into the cell through a liquid nitrogen trap to eliminate condensable impurities. Nitrogen gas was obtained from a commercial cylinder (Linde ultrahigh-pure grade, 99.999%) and carbon monoxide gas was obtained from a cylinder provided by Matheson (CP grade, 99.5%).

A typical example of the decay signals is given in Fig. 2. The vertical axis represents the signal intensity from the preamplifier in units of mV. This example is for the $2\,0_1 \leftarrow 1\,0$

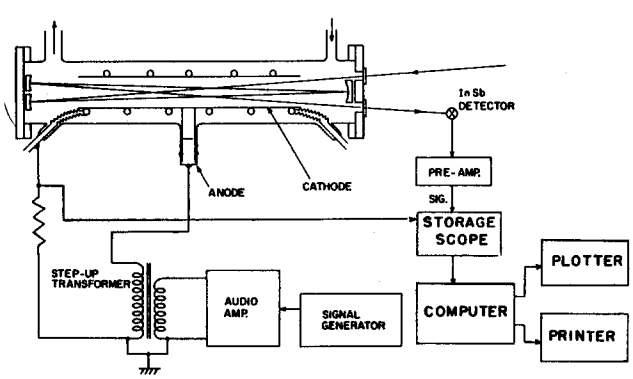

FIG. 1. A schematic diagram of the spectrometer system.

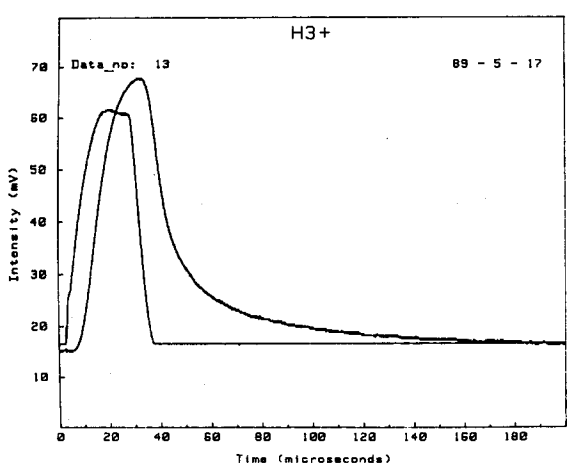

FIG. 2. The transient absorption signal of the $2\,0_1 \leftarrow 1\,0$ transition of the ν_2 fundamental band of H_3^+ (channel a) and the discharge current (channel b) recorded at liquid nitrogen temperature.

transition[20] of the ν_2 fundamental band of H_3^+[21,22] at 2725.898 cm^{-1} recorded at liquid nitrogen temperature. The pressure of H_2 was 300 mTorr. The pathlength was 28.8 m and the peak intensity corresponds to 62% absorption. The second channel shows the current waveform recorded by monitoring the voltage across a 10 Ω resistor inserted between the cathode and the ground. The peak current corresponds to 2.5 A. The rise time of the absorption signal is found to depend on the gas temperature. As the cell temperature gets lower, the pulse duration needs to be longer to reach the steady state intensity. The pulse width was chosen to be long enough for the intensity to reach the steady state (almost).

III. ANALYSIS AND RESULTS

A. Determination of the ion density from the absorption intensity

The decay of an ionic species due to dissociative recombination is described by

$$dN_+/dt = -k_e N_+ N_e, \tag{1}$$

where N^+ and N_e denote the abundances of ions and electrons, respectively. Usually several positive ionic species coexist in discharge plasmas. In some systems, however, only one species is by far the most abundant. In such cases, we can assume $N_+ \sim N_e$ safely. We will discuss the validity of this assumption for each of H_3^+, HN_2^+, and HCO^+. Equation (1) is then written as

$$dN_+/dt = -k_e N_+^2 \tag{2}$$

and the solution is given as

$$1/N_+(t) = 1/N_+(0) + k_e t. \tag{3}$$

As the rotational relaxation time is of the order of 10 ns and the dissociative recombination decay time of the order of 10 μs under the pressure range of our measurements, we can assume that the population of an individual level N_{vJ} is always given by $f_v f_J N_+(t)$ with time-independent $f_v f_J$, where $f_v f_J$ is the fractional population of the level. Under this assumption, Eq. (3) can be rewritten as

$$1/N_{vJ}(t) = 1/N_{vJ}(0) + (k_e/f_v f_J)t. \tag{4}$$

This formulation implicitly assumes that the rate coefficient k_e has little or no rotational dependence. However, this equation will apply even when k_e has a rotational dependence, as long as the rotational relaxation is much faster than the dissociative recombination decay, in which case k_e should be interpreted to be a rotationally averaged value.

The infrared absorption is given in terms of the absorption coefficient as

$$I(\omega,t) = I_c e^{-\alpha(\omega,t)l}, \tag{5}$$

where I_c is the infrared power without absorption and l is the path length. The absorption coefficient is given by

$$\alpha(\omega,t) = \frac{8\pi^2\bar{\mu}^2\omega}{3ch}[N_1(t) - N_2(t)]\phi(\omega), \tag{6}$$

where $\bar{\mu}$ is the dipole matrix element, N_1 and N_2 are the populations of the lower and the upper levels, respectively, and $\phi(\omega)$ is a line shape function defined as

$$\phi(\omega) = \int_{-\infty}^{\infty} L(\omega,v)W(v)dv. \tag{7}$$

In Eq. (7), $L(\omega,v)$ is the Lorentzian line profile function (neglecting the power broadening)

$$L(\omega,v) = \frac{T_2^{-1}}{T_2^{-2} + (\omega - \omega_0 - kv^2)} \tag{8}$$

and $W(v)$ is the Maxwell–Boltzmann velocity distribution function

$$W(v) = \frac{1}{\sqrt{\pi}u} e^{-(v/u)^2}, \tag{9}$$

and

$$u = \sqrt{\frac{2k_B T}{M}} \tag{10}$$

is the most probable velocity. For infrared absorption lines in the 3–4 μm region with reasonably low vibrational temperature as is the case in the present measurements, N_2 is negligible and N_1 is given by $N_1 = f_v f_J N_+$. The abundance is thus calculated from the peak intensity as

$$N_1(t) = \Gamma^{-1}\ln[I_c/I(\omega_0,t)], \tag{11}$$

where Γ is given by

$$\Gamma = \frac{8\pi^2\bar{\mu}^2\omega_0}{3ch}\phi(\omega_0)\cdot l. \tag{12}$$

The simplest approximation in the evaluation of $\phi(\omega_0)$ is the Doppler limit approximation with the Doppler width at the translational temperature. This is the approximation we used in our previous paper.[14] At the Doppler limit, $\phi(\omega)$ becomes a Gaussian profile and Γ is given in terms of the linewidth $\Delta\omega_D$ [half-width at half-maximum (HWHM)]

$$\Gamma = \frac{8\pi^2\sqrt{\pi\ln 2}\bar{\mu}^2\omega_0}{3ch\Delta\omega_D}\cdot l. \tag{13}$$

The Doppler limit approximation, however, should be employed carefully, in particular for heavier molecules at lower temperatures. In this paper, we assumed Eq. (13) and employed the observed effective linewidth rather than the Doppler width, i.e.,

$$\Gamma = \frac{8\pi^2\sqrt{\pi\ln 2}\bar{\mu}^2\omega_0}{3ch\Delta\omega_{\rm eff}}\cdot l \tag{14}$$

The error brought in by this approximation is probably less than a few percent. A more detailed discussion is given in the Appendix.

The transition dipole moment for H_3^+ was calculated from the line strength $S(f-i)$ given in Table II of Miller and Tennyson's paper.[23] For HN_2^+ and HCO^+, the transition dipole moments calculated by Botschwina[24,25] were used and the J-dependent part of the matrix element was as given in Townes and Schawlow's book.[26]

B. The rotational temperature

In our preliminary measurements[14] on H_3^+, the rate coefficient was reported for only one vibration–rotation level (the $J = 3$, $K = 3$ level in the ground vibrational state) and $\Delta\omega_D$ and f_J were evaluated by assuming the translational

and rotational temperatures of 300 K. We extended the measurements to five levels [$(J,K) = (1,0), (1,1), (2,2), (3,3)$, and $(4,4)$] by monitoring the $(2\,0_1 \leftarrow 1\,0)$, $(2\,1_1 \leftarrow 1\,1)$, $(3\,2_{-1} \leftarrow 2\,2)$, $(4\,3_{-1} \leftarrow 3\,3)$, and $(5\,4_{-1} \leftarrow 4\,4)$ transitions to determine the rotational temperature which was necessary to calculate f_J and to examine the rotational dependence of the rate coefficient if any. The population of these five levels at $t = 0$, which was set at the point where the discharge current fell completely to zero, was obtained from Eqs. (11) and (14). Figure 3 shows the plot of log $\{N_{JK}(0)/[g_I(2J+1)]\}$ vs E_{JK} for three different temperatures (i.e., liquid nitrogen, dry-ice, and ice temperature), where g_I is the spin weight. From the slopes, the rotational temperatures were determined to be 120 ± 10, 210 ± 20, and 275 ± 30, respectively. These values are surprisingly low compared with the values generally assumed for glow discharges with He as a buffer gas.[27] Our preliminary measurements[14] were carried out at dry-ice temperature ($-60\,^\circ$C), and assumed that the rotational and translational temperatures were 300 K. From the present measurements, it is now clear that this was too high.

Similarly the rotational temperatures of HN_2^+ and HCO^+ were experimentally determined. The $R(1)$, $P(1)$, $R(5)$, $P(5)$, $R(9)$, and $P(9)$ transitions were measured both for HN_2^+ and HCO^+, and the $R(0)$ line was added in the measurements at liquid nitrogen temperature. In the measurements of HN_2^+ at dry-ice temperature, the $R(17)$ line was added. The rotational temperatures were determined to be 125, 230, and 280 K for HN_2^+ and 120, 230, and 320 K for HCO^+ with about 10% uncertainties. The rotational temperatures for the three ions H_3^+, HN_2^+, and HCO^+ turned out to be slightly different from one another, but the differences may not be significant. The fractional population of each rotational level f_J was calculated based on these rotational temperatures. The partition function was calculated numerically for H_3^+ using the observed[22] and the calculated term values[23] and the approximate analytical expression[26] was used for HN_2^+ and HCO^+.

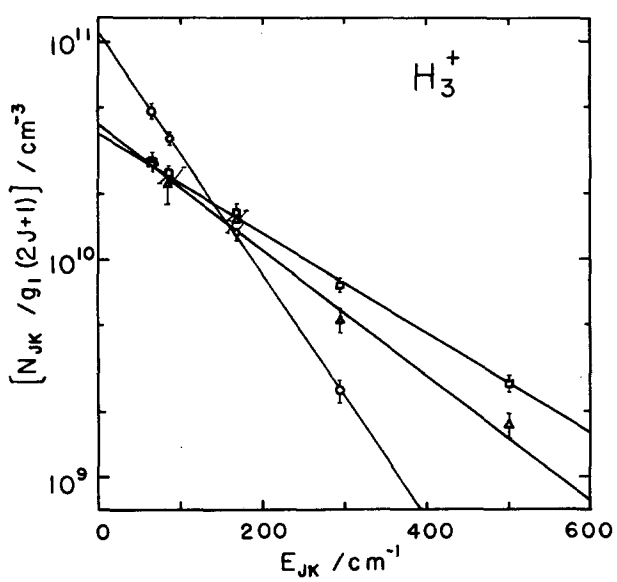

FIG. 3. The relative population of H_3^+ over several rotational levels at "liquid nitrogen temperature" (open circles), at "dry-ice temperature" (open triangles), and at "ice-temperature" (open squares).

The vibrational temperature was estimated to be 500 K from the relative intensity of the hot band from the $v_2 = 1$ state of HN_2^+ with dry-ice cooling, and the f_v values of 1.0, 0.87, and 0.91 were assumed for H_3^+, HN_2^+, and HCO^+, respectively, for the dry-ice and ice-cooled measurements. For the liquid nitrogen-cooled experiments, f_v values of 1.0, 0.96, and 0.98 were assumed for H_3^+, HN_2^+, and HCO^+, respectively. This estimate of the vibrational temperature was made from the relative intensity of the steady-state signals. Therefore, the vibrational temperature may be lower in the afterglow of the pulse discharge employed in the present experiments. The error induced by this approximation is estimated to be less than 5%.

Kim, Theard, and Huntress[28] obtained a very fast rate coefficient for the vibrational relaxation of H_3^+ in H_2 gas to be 3×10^{-10} cm^3 s^{-1}, implying that the vibrational relaxation time of H_3^+ in 300 mTorr of H_2 is of the order of 0.3 μs. This rate is consistent with our observation. The population of H_3^+ in the first excited vibrational state is already smaller by a factor of 100 or more compared with that in the ground state 20–40 μs after the onset of the discharge.

As discussed in the Appendix, the translational temperature of the ions is close to the cell temperature. The electron temperature was not measured in this work. We assumed that the electron temperature is equal to the translational temperature of the ions. The energy loss of electrons of higher energy than about 10 eV can occur through dissociations and ionizations of H_2. The inelastic collisions of electrons with H_2 which lead to the rotational and vibrational excitations are the main energy loss processes of electrons of energy below about 10 eV. The cross section for the rotational excitation is of the order of 1×10^{-17} cm^2 and that for the vibrational excitation is by about an order of magnitude larger,[29] and the energy loss rate coefficients of the electrons of energy of about a few eV due to the rotational and vibrational excitation of H_2 are estimated to be of the order of 10^{-9} and 10^{-8} cm^3 s^{-1}, respectively. Therefore, the electrons are thermalized very rapidly in less than a μs in the pressure range of a few hundred mTorr to 1 Torr of H_2.

It is very interesting to note that the abundance of the ions (H_3^+, HN_2^+, and HCO^+) produced in the hollow cathode does not have a measurable temperature dependence: about the same amount of ions can be generated at ice-cooled temperature as at liquid nitrogen temperature ($\sim5\times10^{11}$ cm^{-3} for H_3^+, $\sim2\times10^{11}$ cm^{-3} for HN_2^+, and $\sim3\times10^{11}$ cm^{-3} for HCO^+). However, we noticed a temperature dependence of the rise time of the absorption signals of all of H_3^+, HN_2^+, and HCO^+. It takes a longer time for the signal to reach the steady-state level at liquid nitrogen temperature than at ice temperature. Because of this, we were misled at one stage to conclude that the ion abundance was less at liquid nitrogen temperature than at ice temperature when the discharge pulse duration was held fixed at 20 μs. We found that the pulse duration of 20 μs was not long enough at liquid nitrogen temperature, although it was long enough for

the absorption intensity to reach a steady state at ice temperature. However, interestingly enough, the steady-state intensity eventually reached the same level when the pulse duration was lengthened to about 40 μs. The explanation of this phenomenon is not clear.

C. Dissociative recombination rate coefficient of H_3^+

The main channel of formation of H_3^+ in hydrogen discharge plasma is

$$H_2 \rightarrow H_2^+, \tag{15}$$

$$H_2 + H_2^+ \rightarrow H_3^+ + H, \tag{16}$$

and the depletion processes are

$$H_3^+ + e^- \rightarrow 3H \tag{17}$$

and

$$H_3^+ + e^- \rightarrow H_2 + H. \tag{18}$$

It is known that the relative abundances of H^+ and H_5^+ are less than a few percent of the total positive ions in the discharge through H_2.[30,31] Because the reaction between H_2^+ and H_2 is very rapid,[30,31] the abundance of H_2^+ is negligibly small under the present experimental conditions. Thus, H_3^+ is by far the dominant positive ion in our hollow cathode discharge and we can assume $N_+ \sim N_e$ in very good approximation.

Figure 4(a) shows an example of the plot of $1/N_+(t)$ obtained from the measured decay curve for the $2\ 0_1 \leftarrow 1\ 0$ transition recorded at liquid nitrogen temperature. This very good linear relationship shows that the decay process is indeed the dissociative recombination. The slope $(4.294 \pm 0.006) \times 10^{-7}\ \mathrm{cm^3\ s^{-1}}$ and the intercept in this example are typical of many runs repeated over the past several months. The statistical uncertainty of the slope is far smaller than the fluctuations observed from one run to another which usually amounted to several percent. Figure 4(b) is the plot of $\log\,[N_+(t)]$ which clearly indicates that the decay is not exponential.

Figure 5 shows the decay of the $4\ 3_{-1} \leftarrow 3\ 3$ transition of H_3^+ with several mTorr of N_2 added to about 500 mTorr of H_2 at dry-ice temperature. The $\log[N_+(t)]$ vs t is given in Fig. 6. In this case, the main loss channel of H_3^+ is the reaction with N_2 and the process is characterized by an exponential decay. The reaction rate obtained from the slope $K = k[N_2] \sim 2.2 \times 10^5\ \mathrm{s^{-1}}$ yields $[N_2] \sim 1.3 \times 10^{14}\ \mathrm{cm^{-3}}$ ($\sim$3.7 mTorr) by using the known value[32] for the reaction rate coefficient $k = 1.7 \times 10^{-9}\ \mathrm{cm^3\ s^{-1}}$. The pressure measurement of N_2 was not made very precisely, because the present gas handling system is not sophisticated enough to warrant a precise mixing of a small amount of N_2 to a large amount of H_2. If the system is improved or premixed gases are prepared, this method is usable to determine reaction rate coefficients. Moreover, this example clearly demonstrates that the processes observed are not instrumental artifacts or diffusion-limited processes.

As it was found[14] that the recombination rate coefficient had no measurable pressure dependence in the pressure range of 0.1–1 Torr, most measurements were carried out in the 200–600 mTorr pressure range. Table I summarizes the

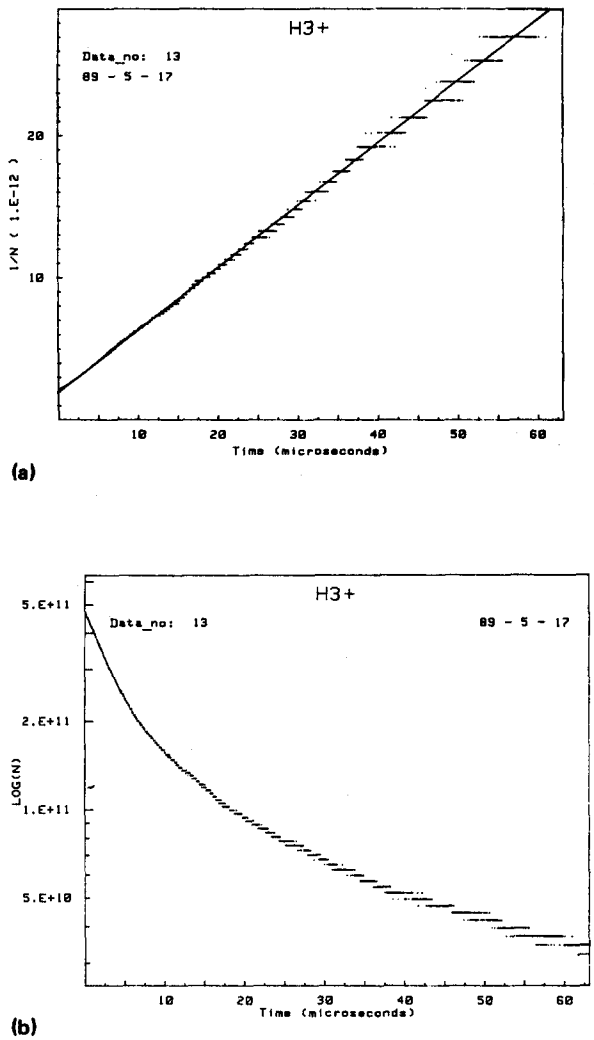

FIG. 4. (a) The $1/N_+(t)$ vs t plot of a decay signal of H_3^+ given in Fig. 2. The origin of the time is taken at the point where the current falls to zero completely. The total H_3^+ abundance at $t = 0$ is found to be about 5×10^{11} $\mathrm{cm^{-3}}$. (b) The $\log\,[N_+(t)]$ plot of the same signal given in Fig. 2.

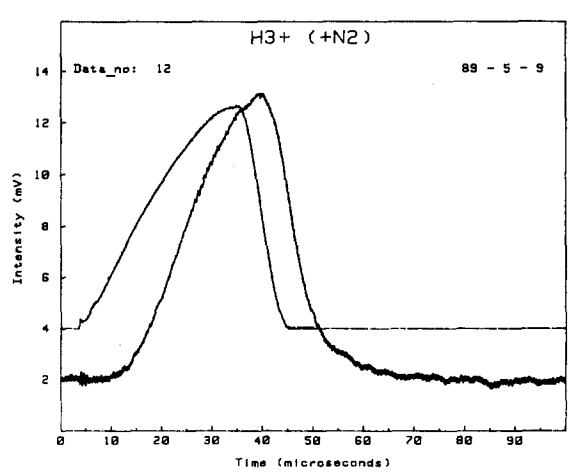

FIG. 5. A decay signal of H_3^+ ($4\ 3_{-1} \leftarrow 3\ 3$ transition) due to the reaction with N_2.

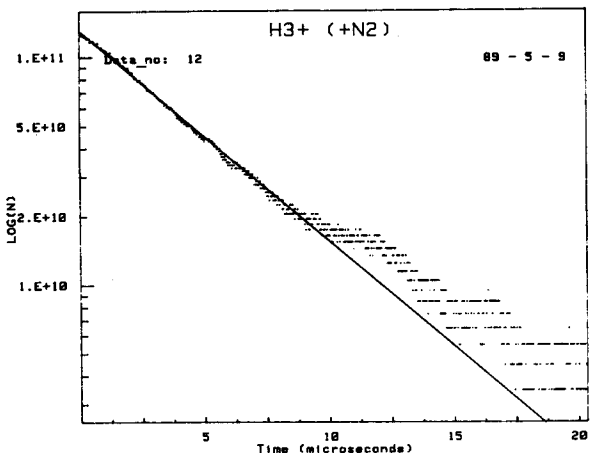

FIG. 6. The log $[N_+(t)]$ plot as a function of time for the signal shown in Fig. 5. The decay is exponential as expected.

rate coefficients thus determined for the five rotational states at three different temperatures. These values were obtained by taking the average of several runs (typically five). The standard deviation amounts from several to 10% which is caused probably by fluctuations of the laser power. The measurements at ice-cooled temperature as well as those for HN_2^+ at liquid nitrogen temperature listed in Table II below were performed with more frequent power measurements between the decay measurements. As a result, a slightly better accuracy was attained.

D. HN_2^+ and HCO^+

The dominant formation processes of HN_2^+ and HCO^+ are

$$H_3^+ + N_2 \rightarrow HN_2^+ + H_2, \quad (19)$$

$$H_3^+ + CO \rightarrow HCO^+ + H_2 \quad (20)$$

and they are depleted by the dissociative recombination with electrons

$$(HN_2^+ \text{ or } HCO^+) + e^- \rightarrow (N_2 \text{ or } CO) + H. \quad (21)$$

Since the proton transfer reaction from H_3^+ to N_2 or CO is very fast, the abundance of H_3^+ in the discharge of hydrogen with 20–30 mTorr of N_2 or CO is negligibly small (20–30 μs) after the discharge is started. Therefore, the approximation $N_+ \sim N_e$ is a very good approximation for both HN_2^+ and HCO^+, and the decay of the absorption signals of HN_2^+ and HCO^+ is described also by Eq. (2). Figure 7 is an example of the HN_2^+ signal [$P(5)$ line[33] at 3252.071 cm^{-1}] recorded at liquid nitrogen temperature. Figure 8 shows the $1/N_+(t)$ plot of the signal given in Fig. 7. From this slope, the dissociative recombination rate coefficient was obtained to be 1.378×10^{-6} $cm^3\,s^{-1}$. Figures 9 and 10 show examples for HCO^+ signal [$R(5)$ line[34] at 3106.0909 cm^{-1}]. The rate coefficient was determined to be 6.04×10^{-7} $cm^3\,s^{-1}$ in this example. Tables II and III summarize the rate coefficients for HN_2^+ and HCO^+ determined here, respectively.

TABLE I. The dissociative recombination rate coefficients of H_3^+ in the ground vibrational state (in units of 10^{-7} $cm^3\,s^{-1}$).

J, K	110 K	210 K	273 K
1, 0	4.1(2)[a]	2.5(1)	1.72(5)
1, 1	4.1(1)	2.7(2)	1.77(10)
2, 2	4.6(4)	2.4(2)	1.85(6)
3, 3	4.5(5)	2.6(2)	1.91(7)
4, 4	···	2.2(2)	1.9(4)

[a] Standard deviation in units of the last quoted digits

TABLE II. Dissociative recombination rate coefficients of HN_2^+ (in units of 10^{-7} $cm^3\,s^{-1}$).

level	transition	110 K	210 K	273 K
$J=0$	$R(0)$	19.8(8)[a]	···	···
$J=1$	$R(1)$	14.6(4)	8.7(2)	7.6(4)
	$P(1)$	14.4(14)	10.6(7)	···
$J=5$	$R(5)$	15.1(5)	···	7.0(9)
	$P(5)$	14.6(8)	···	···
$J=9$	$R(9)$	13.5(14)	8.4(3)	7.0(1)
	$P(9)$	14.9(4)	7.6(2)	6.6(3)
$J=17$	$R(17)$	···	9.7(7)	···
	$P(17)$	···	7.9(2)	···

[a] Standard deviation in units of the last quoted digits.

E. Rotational and temperature dependences

The measurements were repeated several times at the three different temperatures on several different vibration–rotation lines of H_3^+, HN_2^+, and HCO^+ as described above. As summarized in Tables I–III, the measurement accuracy is not good enough to conclude whether there is a rotational dependence of the rate coefficients. As the measurements with better accuracy (H_3^+ at 275 K and HN_2^+ at 110 K) suggest, the rotational dependence is likely to be very small, if any. Moreover, because the rotational relaxation is much faster than the recombination decay, only the rotationally averaged rate coefficient is possible to be observed.

Figure 11 shows the temperature dependence of the rate

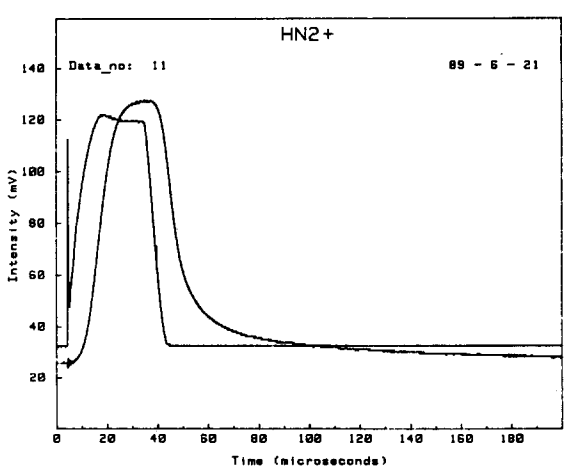

FIG. 7. An example of the HN_2^+ signals [$P(5)$ line at 3252.071 cm^{-1}] recorded with liquid nitrogen cooling.

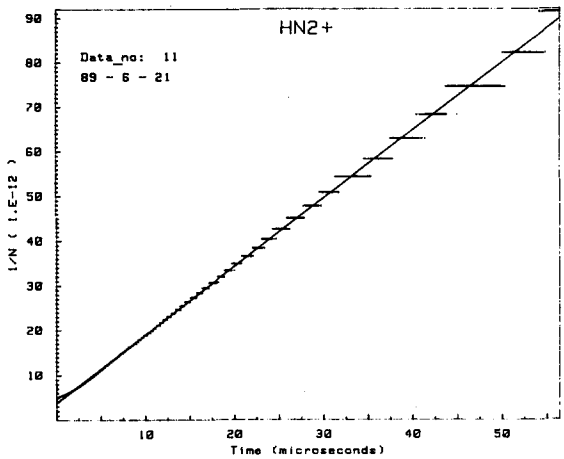

FIG. 8. The $1/N_+(t)$ plot of the signal given in Fig. 7.

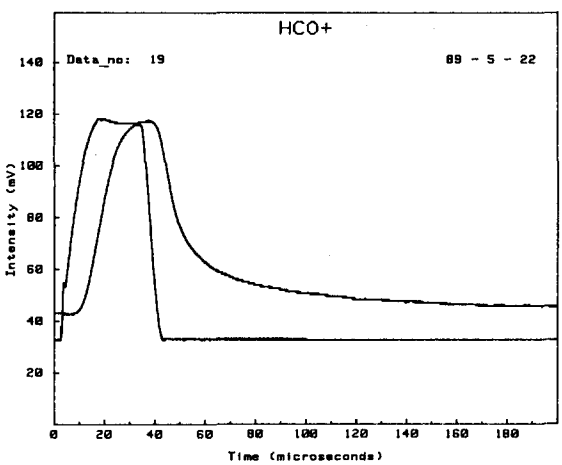

FIG. 9. An example of the HCO^+ signals [$R(5)$ line at 3106.0909 cm^{-1}] recorded with liquid nitrogen cooling.

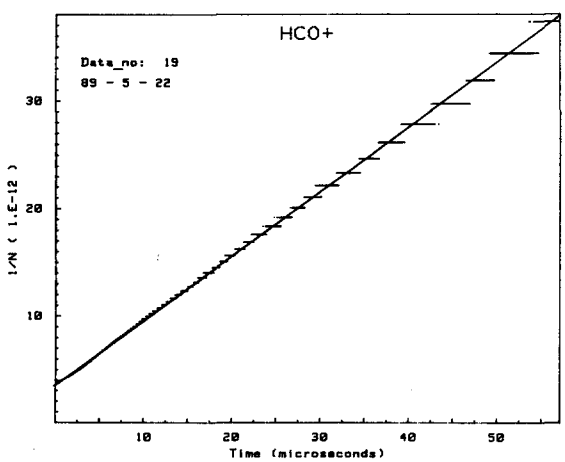

FIG. 10. The $1/N_+(t)$ plot of the signal given in Fig. 9.

TABLE III. Dissociative recombination rate coefficients of HCO^+ (in units of 10^{-7} cm^3 s^{-1}).

level	transition	110 K	210 K	273 K
$J=0$	$R(0)$	6.5(2)[a]	···	···
$J=1$	$R(1)$	5.4(1)	4.6(4)	3.3(1)
$J=5$	$R(5)$	6.0(3)	3.77(4)	3.0(1)
	$P(5)$	5.6(5)	4.2(3)	3.0(2)
$J=9$	$R(9)$	···	3.9(2)	···
	$P(9)$	5.8(2)	···	3.0(1)

[a] Standard deviation in units of the last quoted digits.

coefficients for all the three ionic species. The temperature dependences obtained previously[4,5,16,17] are indicated by broken lines. The temperature dependence measured by Macdonald, Biondi, and Johnsen show a curious deviation from the T^{-1} dependence below about 400 K of electron temperature. Our data suggest that the T^{-1} dependence may extend further toward the lower temperature region. Our data for HCO^+ are consistent with the temperature dependence $T_e^{-0.69}$ obtained by Ganguli *et al.*[16] in the range of $295 < T_e < 5500$ K, and suggest that it can be extrapolated to 100 K. Our measured points for HN_2^+ fall on the line obtained by Mul and McGowan.[17]

IV. DISCUSSION

The dissociative recombination rate coefficient for H_3^+ determined here is in good agreement with the values obtained by the microwave afterglow technique[4,5] and agrees reasonably well with those obtained by the MB method,[7,12] but disagrees with that obtained by Adams, Smith, and Alge.[1–3] Since the dissociative recombination rate constant

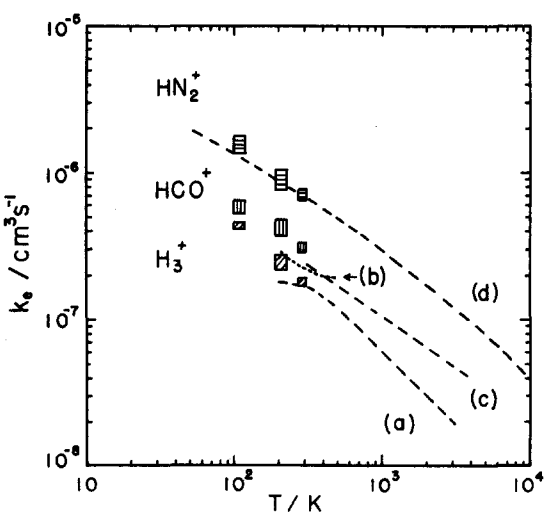

FIG. 11. The temperature dependence of the dissociative recombination rate coefficients for H_3^+, HN_2^+, and HCO^+. Each rectangle represents the measured value and the size reflects the estimate uncertainty. The three entries for each of the three temperatures at which the measurements were carried out are for HN_2^+, HCO^+, and H_3^+ in descending order. The dashed and dotted lines are taken from Ref. 5 for (a), Ref. 4 for (b), Ref. 16 for (c), and Ref. 17 for (d).

for H_3^+ obtained in the present experiment was very different from that obtained by Smith and his co-workers,[1–3] we carefully checked various possibilities which might have caused much faster decay than that observed by Smith and co-workers. One may argue that the decay process observed in our previous experiments[14] as well as in this experiment is not due to the dissociative recombination process, but to other processes such as ambipolar diffusion, reactions with impurities, or collisional-radiative recombination.[35] All these possibilities were carefully examined and all were ruled out as not being processes which might have caused faster decay. Detailed discussions were given in Ref. 14 and only a few more comments will be added here.

The ambipolar diffusion loss rate $D_a p/\Lambda^2$, is estimated to be 50 s^{-1} Torr by assuming $D_a p \sim 500$ $cm^3\,s^{-1}$ Torr[29] and $\Lambda \sim 3$ cm (radius of the cathode). So the ambipolar diffusion loss is negligibly small in the pressure range used in this work. Experimentally it is also clear that the ambipolar diffusion is not a dominant process, since no pressure dependence of the decay rate is observed and $N_+(t)$ did not obey the expontential decay.

The ion density (and also electron density) in our plasma is not very high: $N_+ \sim 5\times 10^{11}$ cm^{-3} at $t=0$ for H_3^+. (There is a typographical error in the caption to Fig. 3 of Ref. 14. The ion abundance at $t=0$ is 3×10^{11} cm^{-3} rather than 3×10^{12} cm^{-3}.) At $T=110$ K and $[e]=3\times 10^{11}$ cm^{-3}, the collisional-radiative recombination rate coefficient is calculated to be 7.4×10^{-7} $cm^3\,s^{-1}$ using Eq. (29) in a paper by Stevefeld, Boulmer, and Delpech[35] derived for transitions between hydrogenic energy levels of high principal quantum number. One may conclude that this mechanism explains the process observed in this experiment. However, this is not the case for two reasons. First, the collisional-radiative recombination rate coefficient has a distinctively different temperature dependence. At $T=210$ K, the rate coefficient would be 4.0×10^{-8} $cm^3\,s^{-1}$ and at $T=275$ K it would be 1.2×10^{-8} $cm^3\,s^{-1}$, which disagree with the experimentl results. Second, if this process is dominant, $1/N_+(t)$ cannot be linear with t. As given in Fig. 4 as an example of the signals taken at $T=110$ K, $1/N_+(t)$ shows a linear dependence on t over an order of magnitude of $N_+(t)$. From these experimental observations, we can conclude that this is not a dominant process of the ion loss in our experiments.

Michels and Hobb's theory[10] which indicated that H_3^+ in the vibrational states below $v=3$ does not undergo rapid dissociative recombination seemed to have provided a solid basis for the argument by Smith and co-workers.[1–3] Another example of the discrepancy between theory and experiment occurs for the dissociative recombination rate of HCO^+. Kraemer and Hazi[36] showed that HCO^+ in the ground vibrational state does not recombine with electrons, implying that the recombination rate coefficient should be very small, based on the noncrossing of the potential curves. Very recently Yousif and Mitchell[37] measured the dissociative recombination rate coefficient of HeH^+ for the first time, showing that the rate is of the order of 10^{-8} $cm^3\,s^{-1}$ contrary to the previously believed value of about 10^{-11} $cm^3\,s^{-1}$.

It is not clear why the FALP measurement yielded such a slow "immeasurable" dissociative recombination rate. Figure 2 of the paper by Adams, Smith, and Alge[1] clearly shows an initial decrease of the electron density in the H_3^+ recombination measurements. They discarded this portion as being caused by the vibrationally excited H_3^+. They cited the detection of CH_3^+ with CH_4 added to H_3^+ flow as evidence of the existence of the vibrationally excited H_3^+. Their observation indicated that less than 5% of the initial products from the reaction between H_3^+ and CH_4 was CH_3^+, suggesting that vibrationally excited H_3^+ could not be the dominant constituent. This observation merely indicates that vibrationally excited H_3^+ existed at the early stage of the reaction, but does not guarantee the persistence of hot H_3^+ further downstream of the flow tube. As described above, our observation implies that the vibrational relaxation is very fast as expected from the rate 3×10^{-10} $cm^3\,s^{-1}$ given by Kim, Theard, and Huntress.[28] Adams, Smith, and Alge did discuss the vibrational relaxation. They chose the relaxation rate coefficient of 1×10^{-10} $cm^3\,s^{-1}$ and the number density of H_2 to be 1×10^{14} cm^{-3} which gave the relaxation time of 0.1 ms. It is stated in the paper that the initial recombination loss lasted for about 0.5 ms. In spite of this estimate which strongly suggests that the vibrational relaxation time was likely to be shorter than its observing time scale (the H_3^+ or D_3^+ was created by adding a relatively large concentration of H_2 or D_2 to the afterglows[1]), they concluded that the observed initial decrease of the electron density was due to the vibrationally excited H_3^+ and the dissociative recombination of the ground H_3^+ was indeed very slow. Although an implication of the argument given above is that the initial decay observed in their experiment is indeed mainly due to H_3^+ in the ground state, there remains a question. The decay became slow somewhat abruptly at the distance $z \sim 50$ cm (see Fig. 2 of Ref. 1) and turned to be diffusion limited afterward. We are not in a position to speculate more based on a figure which does not indicate the accuracy and the reproducibility of the measurements. To unravel this puzzle, one should repeat the FALP experiment or conduct similar measurements.

CONCLUSION

Our spectroscopic measurements have clearly established that the dissociative recombination rate coefficient of H_3^+ in the ground state is not as small as advocated by Smith and co-workers, being in good agreement with the results obtained with the microwave afterglow and other techniques. Measurements have been extended to HN_2^+ and HCO^+, and the rate coefficients obtained are found to be in good agreement with previous results. The measurements were carried out at three different temperatures and the temperature dependence is consistent with that established by the merged beam and microwave afterglow experiments, although our temperature range was rather limited.

ACKNOWLEDGMENTS

I thank Takako Amano for implementing the data-acquisition system and writing an analysis program. I also

gratefully acknowledge R. H. Schwendeman and H. Sasada for providing their Voigt line profile fitting program. I am grateful to J. K. G. Watson for reading the manuscript.

APPENDIX

Although the Voigt line profile can be evaluated only numerically, the peak amplitude $\phi(\omega_0)$ is expressed in a series expansion

$$\phi(\omega_0) = (2/\Delta\omega'_D)\exp(r^2)\cdot\mathrm{erfc}(r), \tag{A1}$$

where $\mathrm{erfc}(r)$ is the error function defined as

$$\mathrm{erfc}(r) = \int_r^\infty e^{-t^2}\,dt = \frac{\sqrt{\pi}}{2} - r\left[1 - \frac{r^2}{3\cdot 1!} + \frac{r^4}{5\cdot 2!} - \frac{r^6}{7\cdot 3!} + \cdots\right]. \tag{A2}$$

In these equations, r is defined as $\Delta\omega_L/\Delta\omega'_D$, where $\Delta\omega_L$ is the Lorentz linewidth and $\Delta\omega'_D$ the Doppler half-width at the $1/e$ point, i.e., $\Delta\omega'_D = \Delta\omega_D/\sqrt{\ln 2}$, where $\Delta\omega_D$ is the Doppler width (HWHM). Although this series converges for any value of r, this form is most suitable for small r. In the regime where r is very large, the following form is more suitable:

$$\exp(r^2)\cdot\mathrm{erfc}(r) = \exp(1/s^2)\cdot\mathrm{erfc}(1/s) = \cfrac{s/2}{1+\cfrac{s^2/2}{1+\cfrac{2s^2/2}{1+\cfrac{3s^2/2}{1+\cfrac{4s^2/2}{1+\cdots}}}}}, \tag{A3}$$

where $s = 1/r$. In the evaluation of $\phi(\omega_0)$, both the Doppler width and the Lorentz widths should be known. Usually fitting the line profile to the Voigt line profile to determine both the Doppler and the Lorentz linewidths is not likely to be successful due to the strong correlation between the two parameters. If the translational temperature is known, as is the case in stable molecules, the Doppler width can be fixed at the calculated value to determine the Lorentz linewidth from a least-squares fit. It was shown in the text that the rotational temperature is close to the cell temperature. This suggests that the translational temperature is assumed to be equal to the cell temperature in good approximation.

Fig. 12 shows a line profile of the $R(5)$ transition of HCO^+ recorded at liquid nitrogen temperature with a discharge in a mixture of 20 mTorr of CO and 300 mTorr of H_2 modulated at 6 kHz frequency. The linewidth (HWHM) of this line is measured to be 75 MHz. HCO^+ is an exceptional case where the Lorentz linewidth has been measured by microwave spectroscopy.[38] A least-squares fit to a Voigt line profile yielded the Doppler width of 66.0(1.5) MHz and the pressure broadening of 16.0(1.5) MHz (with the standard deviation in parentheses). The Doppler width determined corresponds to the width expected for a translational temperature of 110 K. The pressure broadening parameter obtained here is considerably larger than that obtained by Anderson *et al.*,[38] $\Delta\nu_L/p = 30$ MHz/Torr. If the Lorentz width was fixed at 9 MHz as obtained by Anderson *et al.*, fitting to the Voigt line profile yielded the Doppler width of 70.8(0.9) MHz with somewhat worse quality of fit. The Doppler width corresponds to the translational temperature of 130 K which is slightly higher than the rotational temperature. Since there is a large correlation between the Doppler width and the Lorentz width, it may be premature at this stage to conclude that the pressure broadening of HCO^+ is larger than that obtained previously.

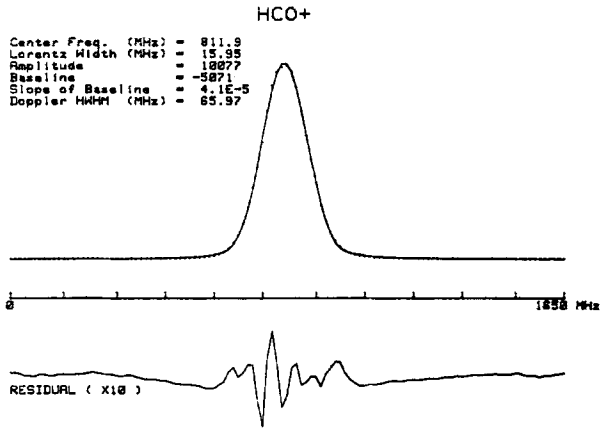

FIG. 12. The observed and calculated line profiles of $R(5)$ transition of HCO^+. The line profile was recorded by stepping the laser frequency and is indicated by dots. The calculated points are connected by solid lines. The residuals between the observed and the calculated are given as the bottom trace. Both amplitude and frequency instabilities of the laser are the dominant sources of the deviations.

In the evaluation of the peak intensity, we assumed Eq. (14) and employed the observed effective linewidth rather than the Doppler width as the input parameter. If the effective linewidth is defined by

$$\Delta\omega_{\mathrm{eff}} = \Delta\omega_D \exp(-r^2)\left[1 - (2/\sqrt{\pi}) \times r\left\{1 - \frac{r^2}{3\cdot 1!} + \frac{r^4}{5\cdot 2!} - \frac{r^6}{7\cdot 3!} + \cdots\right\}\right]^{-1}, \tag{A4}$$

then Eq. (14) is correct for any $\Delta\omega_D$ and $\Delta\omega_L$, but it does not lead to a conclusion than $\Delta\omega_{\mathrm{eff}}$ is the linewidth of a Voigt line profile. When the deviation from the Doppler line profile is not so large, $\Delta\omega_{\mathrm{eff}}$ may be interpreted to be the linewidth. In the example of HCO^+ given above, the observed Doppler and Lorentz widths yield the effective half-width of 75 MHz using Eq. (A4) which agrees very well with the observed width. The error brought in by this approximation is expected to be less than a few percent.

[1]N. G. Adams, D. Smith, and E. Alge, J. Chem. Phys. **81**, 1778 (1984).
[2]D. Smith and N. G. Adams, Astrophys. J. Lett. **284**, L13 (1984).
[3]N. G. Adams and D. Smith, in *Astrochemistry. IAU Symnposium No. 120*, edited by M. S. Vardya and S. P. Tarafdar (Reidel, Dordrecht, 1987).
[4]M. T. Leu, M. A. Biondi, and R. Johnsen, Phys. Rev. A **8**, 413 (1973).
[5]J. A. Macdonald, M. A. Biondi, and R. Johnsen, Planet. Space Sci. **32**, 651 (1984).
[6]B. Peart and K. T. Dolder, J. Phys. B **7**, 1948 (1974).
[7]D. Auerbach, R. Cacak, R. Caudano, T. D. Gaily, C. J. Keyser, J. Wm. McGowan, J. B. A. Mitchell, and S. F. J. Wilk, J. Phys. B **10**, 3797 (1977).

[8]J. Wm. McGowan, P. M. Mul, V. S. D'Angelo, J. B. A. Mitchell, P. Defrance, and H. R. Froelich, Phys. Rev. Lett. **42**, 373 (1979).
[9]D. Mathur, S. U. Khan, and J. B. Hasted, J. Phys. B **11**, 3615 (1978).
[10]H. H. Michels and R. H. Hobbs, Astrophys. J. Lett. **286**, L27 (1984).
[11]H. Hus, F. Youssif, A. Sen, and J. B. A. Mitchell, Phys. Rev. A **38**, 658 (1988).
[12]J. B. A. Mitchell, C. T. Ng, L. Forand, R. Janssen, and J. Wm. McGowan, J. Phys. B **17**, L909 (1984).
[13]R. Johnsen, Int. J. Mass Spectrom. Ion. Proc. **81**, 67 (1987).
[14]T. Amano, Astrophys. J. Lett. **329**, L121 (1988).
[15]M. T. Leu, M. A. Biondi, and R. Johnsen, Phys. Rev. A **8**, 420 (1973).
[16]B. Ganguli, M. A. Biondi, R. Johnsen, and J. L. Dulaney, Phys. Rev. A **37**, 2543 (1988).
[17]P. M. Mul and J. Wm. McGowan, Astrophys. J. Lett. **227**, L157 (1979).
[18]T. Amano, J. Opt. Soc. Am. B **2**, 790 (1985).
[19]T. Amano and K. Tanaka, J. Chem. Phys. **83**, 3721 (1985).
[20]We adopt the notation used by Miller and Tennyson. The quantum numbers in the upper state express *J*, *G*, and *U*. The definition of *G* and *U* is as given by Watson. The quantum numbers in the lower state are as usual *J* and *K*.
[21]T. Oka, Phys. Rev. Lett. **45**, 531 (1980).
[22]J. K. G. Watson, S. C. Foster, A. R. W. McKellar, P. F. Bernath, T. Amano, F. S. Pan, M. W. Crofton, R. S. Altman, and T. Oka, Can. J. Phys. **62**, 1875 (1984).
[23]S. Miller and J. Tennyson, Astrophys. J. **335**, 486 (1988).
[24]P. Botschwina, Chem. Phys. Lett. **107**, 535 (1984).
[25]P. Botschwina, in *Ion and Cluster Ion Spectroscopy and Structure*, edited by J. P. Maier (Elsevier, Amsterdam, 1989), pp. 59–108.
[26]C. H. Townes and A. L. Schawlow, *Microwave Spectroscopy* (McGraw–Hill, New York, 1955).
[27]See, e.g., F. Pan and T. Oka, Phys. Rev. A **36**, 2297 (1987).
[28]J. K. Kim, L. P. Theard, and W. T. Huntress, Int. J. Mass Spectrom. Ion Phys. **15**, 223 (1974).
[29]A. von Engel, *Electric Plasmas: Their Nature and Uses* (Taylor and Francis, New York, 1983).
[30]M. Saporoschenko, Phys. Rev. A **139**, 349 (1965).
[31]D. L. Albritton, T. M. Miller, D. W. Martin, and E. W. McDaniel, Phys. Rev. **171**, 94 (1968).
[32]See, e.g., J. K. Kim, L. P. Theard, and W. T. Huntress, Chem. Phys. Lett. **32**, 610 (1975).
[33]J. C. Owrutsky, C. S. Gudeman, C. C. Martner, L. M. Tack, N. H. Rosenbaum, and R. J. Saykally, J. Chem. Phys. **84**, 605 (1986).
[34]T. Amano, J. Chem. Phys. **79**, 3595 (1983).
[35]J. Stevefelt, J. Boulmer, and J-F. Delpech, Phys. Rev. A **12**, 1246 (1975).
[36]W. P. Kraemer and A. U. Hazi, in *Molecular Astrophysics: State of the Art and Future Directions*, edited by G. H. F. Diercksen, W. F. Huebner, and P. W. Langhoff (Reidel, Dordrecht, 1985).
[37]F. B. Yousif and J. B. A. Mitchell, Phys. Rev. A **40**, 4318 (1989).
[38]T. G. Anderson, C. S. Gudeman, T. A. Dixon, and R. C. Woods, J. Chem. Phys. **72**, 1332 (1980).